

Complementarity Reveals Bound Entanglement of Two Twisted Photons

Beatrix C. Hiesmayr

*Institute of Theoretical Physics and Astrophysics,
Masaryk University, Kotlářská 2, 61137 Brno, Czech Republic and
University of Vienna, Faculty of Physics, Boltzmanngasse 5, A-1090 Vienna, Austria*

Wolfgang Löffler

Leiden University, Quantum Optics & Quantum Information, PO Box 9500, 2300 RA Leiden, Netherlands

We witness for the first time the generation of bound entanglement of two photon qutrits, whose existence has been predicted by the Horodecki family in 1998. Detection of these heavily mixed entangled states, from which no pure entanglement can be distilled, is possible using a key concept of Nature: complementarity. This captures one of the most counterintuitive differences between a classical and quantum world, for instance, the well-known wave-particle duality is just an example of complementary observables. Our protocol uses *maximum* complementarity between observables: the knowledge about the result of one of them precludes any knowledge about the result of the other. It enables ample detection of entanglement in arbitrary high-dimensional systems, including the most challenging case, the detection of bound entanglement. For this we manipulate “twisted” twin photons in their orbital angular momentum degrees of freedom. Our experimentally demonstrated “*maximum complementarity protocol*” is very general and applies to all dimensions and arbitrary number of particles, thus enables simple entanglement testing in high-dimensional quantum information and opens up the quest of understanding the meaning of this type of entanglement in Nature.

The boundary between a classical and quantum world is the domain of mixed quantum states. Quantum entanglement of mixed states is much more complex than that of pure states and subject of intense research. In 1998 it was found that entanglement of mixed states is not “flat”, but has an intriguing structure:¹ Entangled quantum states can be classified into two distinct types, those that can and those that cannot be distilled into pure entangled states using statistical local operations and classical communication. Undistillable entangled states are called bound entangled. Bound entanglement can occur in bipartite systems with dimensions larger than $d = 2$ or in the case of more particles. These two different types of bound entanglement differ considerably. The case of more than 2 entangled qubits has recently been discovered experimentally in photonic multipartite systems,^{2–4} trapped ions,⁵ NMR,⁶ further, there is one study in a continuous-variable context.⁷ These results on multipartite qubit bound entanglement became already interesting for certain quantum information tasks such as steering⁸ and reduction of the communication complexity.⁹ We investigate here the case of bound entanglement of *only two* photonic qutrits ($d = 3$) using the orbital angular momentum degree of freedom of light; this is the simplest case of bound entanglement and complications such as occurring for multipartite systems¹⁰ do not occur. The orbital angular momentum of photons^{11,12} is used in a number of studies to obtain high-dimensional bipartite entangled qudits,^{13–16} apart from fundamental questions such as those discussed here, the system shows promise in quantum cryptography¹⁷ due to improved security, increased resistance against noise, and higher bit rates^{18–20} compared to qubits. In particular for such

higher-dimensional qudit systems, it is well known that it is extremely hard to check whether a given state, especially if it is mixed – the daily situation in a laboratory – is separable or entangled. There are several operational criteria available to detect entanglement, where the most famous and powerful one is the Peres-Horodecki criterion, which is based on the partial transposition in one subsystem.^{21,22} After partial transposition, either all eigenvalues remain positive (PPT), or in the other case, if at least one eigenvalue is found to be negative, the state is entangled. The transposition of a state is synonymous to time reversal,²³ so PPT tests if a state where time’s arrow is reversed for one of its partitions is still a physical state: obviously, if the state is separable, this must be the case. For two qubits, the reverse is also true and PPT is a sufficient criterion for separability. This argument fails already for two qutrits, where it turns out that bound entangled qutrits are PPT. This brings us back to distillability: it was found that it is actually the positivity under partial transposition, which makes bound entangled states undistillable.¹ In the experiment described here, in a first step, we produce photon states that are bound entangled in their orbital angular momentum degree of freedom and verify the positivity under partial transposition via state tomography. In a second step we apply the maximum complementarity protocol using sets of observables, for which their eigenbases are mutually unbiased, to witness directly the inseparability of two bound entangled qutrits.

The Maximum Complementarity Protocol: Consider the following scenario of a source producing two-qudit states $\rho \in \mathbb{C}^{d \times d}$, namely quantum states with d


"The Maximum Complementarity Protocol"			
			
1. Step	Outcomes of Observable A_1 $\{0_1, 1_1, \dots, (d-1)_1\}$	Outcomes of Observable B_1 $\{0_1, 1_1, \dots, (d-1)_1\}$	Correlation functions: $C_{A_1, B_1} = \sum_{i=0}^{d-1} \text{Tr}(i_1 i_1\rangle\langle i_1 i_1 \rho_d)$
2. Step	Outcomes of Observable A_2 $\{0_2, 1_2, \dots, (d-1)_2\}$	Outcomes of Observable B_2 $\{0_2, 1_2, \dots, (d-1)_2\}$	$C_{A_2, B_2} = \sum_{i=0}^{d-1} \text{Tr}(i_2 i_2\rangle\langle i_2 i_2 \rho_d)$
\vdots	\vdots	\vdots	\vdots
(d+1). Step	Outcomes of Observable A_{d+1} $\{0_{d+1}, 1_{d+1}, \dots, (d-1)_{d+1}\}$	Outcomes of Observable B_{d+1} $\{0_{d+1}, 1_{d+1}, \dots, (d-1)_{d+1}\}$	$C_{A_{d+1}, B_{d+1}} = \sum_{i=0}^{d-1} \text{Tr}(i_{d+1} i_{d+1}\rangle\langle i_{d+1} i_{d+1} \rho_d)$
			$I_{d+1} = \sum_{k=0}^{d-1} C_{A_k, B_k} \leq 2$

FIG. 1. This figure illustrates the steps involved in the complementarity protocol for entanglement detection of bipartite qudits: Alice and Bob determine the experimental probability (coincidence counts) for each detection state, and that for all (mutually unbiased) bases. It is then simply a matter of summing up these probabilities, if the sum is > 2 , the state is entangled. Note that both Alice and Bob are allowed to relabel their measurement outcomes per basis, in order to optimize the detection ability.

degrees of freedom per qudit. Both experimenters, Alice and Bob, can choose among k different observables. What is the best strategy for Alice and Bob to detect the inseparability? The most striking difference between entanglement and separability are revealed by correlations in different basis choices. A fully correlated system is a physical system for which we can predict with certainty the outcome of a second measurement when we know the outcome of a first measurement, opposite to the other extreme case when knowledge of the first measurement outcome does not reveal any information about the second measurement outcome. This we would call a fully uncorrelated system. Let us quantify this statement via a correlation function for two observables given in the spectral decomposition, A_k and B_k measured by Alice and Bob (with respective eigenvectors $\{|i_k\rangle\} = \{|0_k\rangle, \dots, |d-1_k\rangle\}$) by summing all *joint probabilities* $P_{A_k, B_k}(i_k, i_k)$ when both parties have the same outcome i_k

$$C_{A_k, B_k} = \sum_{i=0}^{d-1} P_{A_k, B_k}(i_k, i_k) = \sum_{i=0}^{d-1} \text{Tr}(|i_k i_k\rangle\langle i_k i_k| \rho_d) \quad (1)$$

Here, we allow Alice and Bob to relabel their outcomes such that C gets maximal. Indeed the above function is a *mutual predictability*, since if the state is fully correlated then the outcomes can always be labelled such that $C = 1$ and if fully uncorrelated then any relabeling can only give $C = 1/d$ since all d outcomes are equally likely. However, this function does not tell us anything about entanglement, since clearly the socks of Prof. Bertlmann,²⁴ who has the habit of wearing differently coloured socks, are also fully correlated. Therefore, in a second step, Alice and Bob will now use the fundamental concept of com-

plementarity and choose a second set of observables that are mutually unbiased to the first choices of observables A_1 and B_1 , namely the observables A_2 and B_2 . One way to phrase Bohr's complementarity of two observables A_1 , A_2 is to say that they are non-degenerate; i.e., they do not share any common eigenvector. This implies that the uncertainties of the outcomes are bounded by the scalar product of the eigenvectors of both observables and it is maximal if (and only if) all scalar products satisfy

$$|\langle i_n | j_m \rangle|^2 = \frac{1}{d} \quad \forall i, j \in \{0, 1, \dots, d-1\}. \quad (2)$$

Thus, predictabilities of a product state $|0_1 0_1\rangle$ are given by

$$\begin{aligned} P_{A_1, B_1}(i_1, i_1) &= \delta_{i,0} \\ P_{A_2, B_2}(i_2, i_2) &= \text{Tr}(|i_2 i_2\rangle\langle i_2 i_2| 0_1 0_1) \langle 0_1 0_1| \\ &\stackrel{\text{Eq. (2)}}{=} \underbrace{|\langle 0_1 | i_2 \rangle|^2}_{\frac{1}{d}} \cdot \underbrace{|\langle 0_1 | i_2 \rangle|^2}_{\frac{1}{d}} = \frac{1}{d^2}, \end{aligned} \quad (3)$$

which holds for all i and we obtain for the correlation functions $C_{A_1, B_1} = 1$ and $C_{A_2, B_2} = \frac{1}{d}$. For a third choice of mutually complementary observables we obtain again $\frac{1}{d}$. In general, by adding up m correlation functions we obtain

$$I_m := \sum_{k=1}^m C_{A_k, B_k} \leq 1 + (m-1) \frac{1}{d} \quad (4)$$

that has to hold for all pure separable states. In Ref.²⁵ we have shown that it is also valid for all mixed separable states. Therefore, I_k serves as a detection function of entanglement if and only if the bound is not satisfied. The existence of complete sets of mutually unbiased bases in arbitrary dimensions is an open problem, but in the case of prime-power dimensions d it is known to be $d+1$, leading to

$$I_{d+1} \stackrel{\text{Eq. (4)}}{=} \sum_{k=1}^{d+1} C_{A_k, B_k} \leq 2. \quad (5)$$

It was shown that this detection criterion is very powerful as it e.g. detects all the entanglement of isotropic states and more entanglement of multiparticle Aharanov state than the powerful criteria of Refs. [26–28]. Let us remark that our method of maximum complementarity provides a test for non-separability of a state whereas Bell inequalities can serve as an entanglement test but are designed to test for local realism. Indeed, so far only multipartite bound entangled states were found to violate a Bell inequality while the question is still open for bipartite bound entangled states.

Now, we demonstrate both theoretically and experimentally that I_{d+1} is also capable of detecting bound entanglement for a certain class of so-called magic simplex states or Bell-diagonal states in 3×3 dimensions.

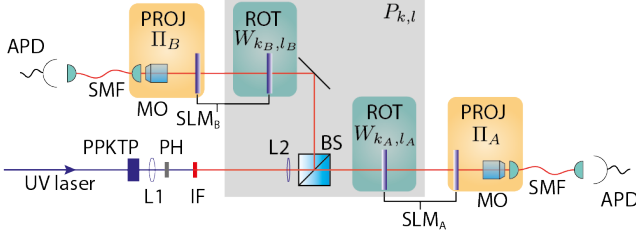


FIG. 2. Experimental setup for generation of bound-entangled bipartite qutrits. Photon pairs are created by downconversion (type-I) of 413 nm UV photons in a PPKTP crystal, momentum-filtered by pinhole (PH), and split probabilistically using a beamsplitter (BS). Rotation (ROT) in the orbital angular momentum superposition mode-space for production of the Bell states $P_{k,l}$ (gray box) via $W_{k_{A/B},l_{A/B}}$ is performed using a spatial light modulator (SLM). Projective measurements (PROJ) are done by appropriate mode transformation and subsequent imaging onto the core of a single mode fibre (SMF) as indicated by $\Pi_{A/B}$. We have implemented both operations on the same SLM. The photons are guided to an avalanche photo diode (APD), and detection events belonging to a single photon pair are post-selected by coincidence detection.

For the experimental test, we have chosen to use orbital-angular-momentum¹¹ (OAM) entangled photons generated by spontaneous parametric downconversion (SPDC). OAM entanglement^{13,14,29,30} is one implementation of spatial entanglement which is particularly intuitive because the quantum correlations of the photon pair are determined only by conservation of orbital angular momentum during pair generation: The OAM ℓ_A and ℓ_B of the downconverted photons must fulfil $\ell_A + \ell_B = 0$ if the pump is a flat (Gaussian) beam with $\ell = 0$.^{13,31} In the OAM basis $|\ell_A, \ell_B\rangle$ the two-photon qutrit state as produced by the crystal is

$$|\Psi_{SPDC}\rangle = \frac{1}{\sqrt{3}} \{ |-1, +1\rangle + |0, 0\rangle + |+1, -1\rangle \}. \quad (6)$$

In the following, we denote the states $\{|\ell = -1\rangle, |\ell = 0\rangle, |\ell = +1\rangle\}$ by $\{|0\rangle, |1\rangle, |2\rangle\}$. As a starting point we take the maximally entangled Bell state $P_{0,0} = |\Psi_{SPDC}\rangle\langle\Psi_{SPDC}|$ and, via applying the unitary Weyl operators $W_{k,l} := \sum_{n=0}^{d-1} e^{\frac{(2\pi i)(kn)}{d}} |n\rangle\langle n+l|$ in one subsystem (e.g. on the photon of Alice), we can synthesize the $d^2 - 1$ maximally entangled Bell states $P_{k,l} = W_{k,l} \otimes \mathbb{1} P_{0,0} W_{k,l}^\dagger \otimes \mathbb{1}$. Any convex combination of these d^2 Bell states forms a so called “magic simplex”³² $\mathcal{W} := \{\rho_d = \sum_{k,l=0}^{d-1} c_{k,l} P_{k,l} | c_{k,l} \geq 0, \sum_{k,l=0}^{d-1} c_{k,l} = 1\}$. This reduced state space of locally maximally mixed states admits a simple geometrical representation (the vertices are the d^2 Bell states) and has been shown^{32–35} to be

powerful in addressing inseparability issues and quantum information theoretic questions.

For our purpose let us reduce the $d^2 - 1$ dimensional parameter space to three (four in case of $d > 3$) parameters q_i and consider the following family of states:

$$\begin{aligned} \rho_d = & \left(1 - \frac{q_1}{d^2 - (d+1)} - \frac{q_2}{d+1} - q_3 - (d-3)q\right) \frac{1}{d^2} \mathbb{1}_{d^2} \\ & + \frac{q_1}{d^2 - (d+1)} P_{0,0} + \frac{q_2}{(d+1)(d-1)} \sum_{i=1}^{d-1} P_{i,0} \\ & + \frac{q_3}{d} \sum_{i=0}^{d-1} P_{i,1} + (1 - \delta_{d,3}) \frac{q_4}{d} \sum_{z=2}^{d-2} \sum_{i=0}^{d-1} P_{i,z} \end{aligned} \quad (7)$$

This family also includes for $d = 3$ the one-parameter Horodecki-state, the first found bound entangled state.¹ Namely, for $q_1 = \frac{30-5\lambda}{21}$, $q_2 = -\frac{8\lambda}{21}$, $q_3 = \frac{5-2\lambda}{7}$ with $\lambda \in [0, 5]$. This state is PPT for $\lambda \in [1, 4]$ and was shown to be bound entangled for $\lambda \in \{3, 4\}$.

Generation of the states ($d = 3$): By expressing the totally mixed state $\mathbb{1}_9$ as the sum of all Bell states $\sum P_{k,l}$ we find that all 9 Bell states need to be mixed to synthesize the state ρ_3 . Note that there are 72 unitary equivalent possibilities³² to generate ρ_3 that we will exploit to deduce the error (see supplementary information). We introduce a measurement-based scheme to produce these mixed states similar to the authors in Refs.^{2–4,36,37} for polarization but in our case for OAM qutrits using spatial light modulation, see Fig. 2. As described above we have to apply single-qutrit rotations (e.g., on qutrit A) using the Weyl matrix $W_{k,l}$ to transform $P_{0,0}$ into any of the 8 other maximally entangled Bell states $P_{k,l}$. This operation is implemented on the spatial light modulators (SLMs, see Fig. 2), which allows us to generate the mixed state by time-multiplexing of the rotation operators $W_{k,l}$ for a particular choice of q_i . Our method is physically equivalent to tracing over a separate degree of freedom to create decoherence, such as the spectral one, a method which has also been used to generate mixed states^{38,39} or stochastic rotation with an additional optical element.^{2–4,36,37} In our case we extend this to obtain full control over the high-dimensional mixture by using *retroactive mixing*: we record photon counts for each of the states $P_{k,l}$, and form the incoherent summation in a computer afterwards. This allows us to explore the magic simplex \mathcal{W} completely, while still obtaining exactly the same result as if mixing would happen during the photon counting time. Projective measurements are performed by mode-conversion on the spatial light modulator and imaging onto a single-mode fibre.

State Tomography and Magic Simplex: We first perform quantum state tomography⁴⁰ of the bound entangled state. We keep $q_3 = -0.5776$ fixed, this allows us to visualize quantum state properties in 2D: Fig. 3

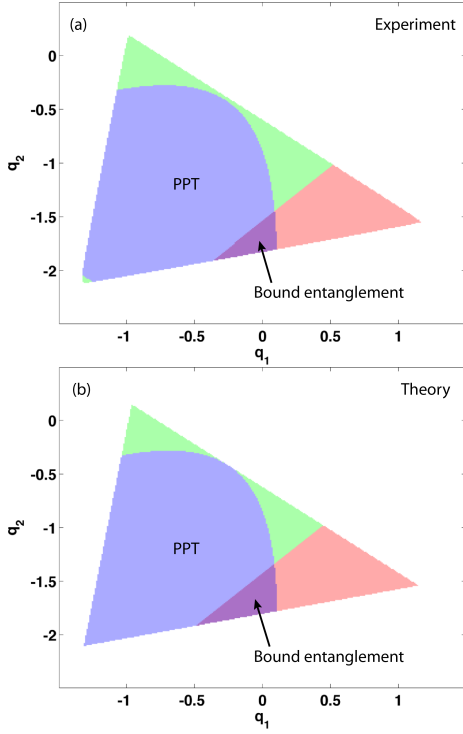


FIG. 3. Experimental (a) and theoretical (b) 2D slice $\{q_1, q_2\}$ through the magic simplex for fixed $q_3 = -0.5776$. All coloured points correspond to states having positive semidefinite eigenvalues, therefore representing physical states. The blue area (curved region) covers the range of states with a positive partial transpose (PPT). The red triangular area indicates where the maximum complementarity protocol applied to the experimentally generated states (a) or theoretical states (b) is greater than 2, thus detecting entanglement. States where all three conditions are fulfilled are bound entangled. We see that the experimental and theoretical geometries agree very well.

shows experimental (a) and theoretical case (b), where each coloured pixel $\{q_1, q_2\}$ corresponds to a state, blue if PPT (curved region), and red if the state violates the maximum complementarity protocol, $2 - I_{d+1} < 0$ (triangle). In regions where all conditions are fulfilled, we have non-separable states with a positive partial transposition, i.e. bound entanglement. We find that, compared to the total area of physical states, the bound entangled states occupy a significant space in the chosen slice through the magic simplex; the extension along q_3 turns out to be even much larger, i.e., the bound entangled states occupies a rather large volume. Since the regions in Fig. 3 are continuous (“they do not have holes”), it is obvious from the geometry that states within the region where all criteria apply are bound entangled. However, it is important to check that the conditions are also fulfilled significantly.¹⁰ In contrast to the polarization qubit case,² in spatial entanglement, the most important errors are due to unwanted rotations of the state due to wavefront aberrations. To quantify these errors, we have

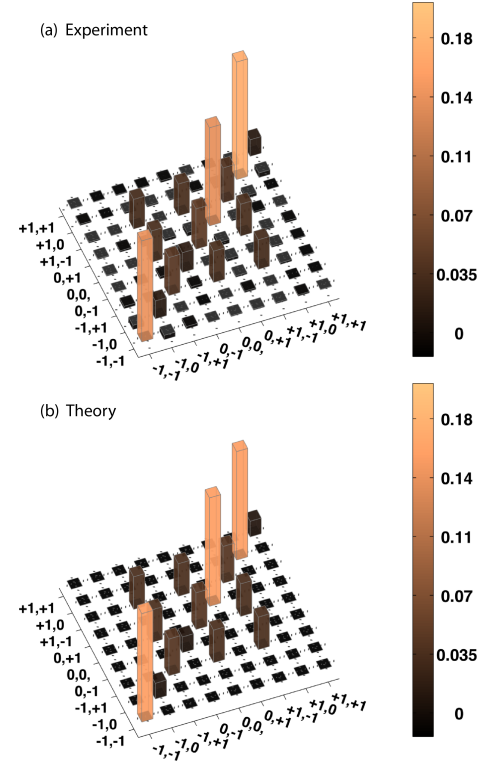


FIG. 4. Experimental (a) and theoretical (b) real parts of the density matrices of the bound entangled state ($q_1 = -0.07$, $q_2 = -1.73$, $q_3 = -0.5774$). The fidelity of the experimental state is 0.98, the complementarity protocol applied to the experimental state gives $2 - I_{d+1} = -0.032 \pm 0.003$ and the minimum eigenvalue of the partially transposed state is $\text{Min}[\text{eig}(\rho^{TA})] = +0.0101 \pm 0.0017$; the state is bound entangled. It is expected to be purely real; the experimental imaginary parts are all below 10%. The axes labels indicate the OAM quantum numbers ℓ .

determined for all 72 unitary-equivalent states of ρ_3 (see supplementary information) the result of the complementarity protocol $2 - I_{d+1}$ and the smallest eigenvalue of the partially transposed state $\text{Min}[\text{eig}(\rho^{TA})]$. This allows us to derive realistic error estimates. In Fig. 4 we plot explicitly the matrix elements of the bound entangled state ($q_1 = -0.07$, $q_2 = -1.73$, $q_3 = -0.5774$) together with the theoretical prediction. The numerical values are $2 - I_{d+1} = -0.032 \pm 0.003$ and $\text{Min}[\text{eig}(\rho^{TA})] = +0.0101 \pm 0.0017$. This clearly proves that the state is bound entangled: non-separable, but PPT.

We studied also the historical Horodecki-state,¹ and we can indeed experimentally confirm bound entanglement thereof for a large range of the λ -parameter. For instance, for $\lambda = 3.5$, we get $2 - I_{d+1} = -0.025 \pm 0.003$, and $\text{Min}[\text{eig}(\rho^{TA})] = +0.012 \pm 0.002$.

Maximum Complementarity Protocol: In a next step we want to verify entanglement of the state, shown in Fig. 4, directly by using the complementarity

protocol. For that, the correlation functions had to be measured directly, which is considered to be difficult due to normalization: In quantum state tomography, proper normalization is imposed during numerical search; here we have to obtain probabilities directly from experimental coincidence rates. We obtain the probabilities P from the normalized coincidence rates Γ via $P_{A_k, B_k}(i_k, i_k) = \Gamma_{A_k, B_k}(i_k, i_k) / \sum_{s_k, t_k} \Gamma_{A_k, B_k}(s_k, t_k)$. From this we calculate the correlation functions C and obtain:

Correlation function	Theory	Experiment
C_{A_1, B_1}	0.675	0.667 ± 0.005
C_{A_2, B_2}	0.468	0.463 ± 0.005
C_{A_3, B_3}	0.468	0.469 ± 0.005
C_{A_4, B_4}	0.468	0.467 ± 0.005
$2 - (I_4 = \sum_k C_{A_k, B_k})$	-0.079	-0.066 ± 0.02

The uncertainties are determined from multiple experimental runs. Experiment and theory agree well, the maximum complementarity protocol confirms that we detect a truly entangled state. In literature, criteria for entanglement are usually applied on density matrices (as we did in the first step). We have performed extensive experimental tests and conclude that the maximum complementarity protocol can directly be measured if the experiment is well under control. This implies a significant advance in the exploration of high-dimensional entangled photons, since the experimental and computational complexity is strongly reduced: We need $N_{QST} = d^2 - 4d^3 + 4d^4$ measurements for (over-complete) state tomography, and only $N_{MCP}^{(1)} = d + d^2$ measurements to determine the function I_{d+1} directly (without normalization), and $N_{MCP}^{(2)} = d^2 + d^3$ including normalization.

Generality of the Maximum Complementarity Protocol: Let us discuss what we would expect for the case of higher dimensional OAM entangled photons in the state ρ_d . We search the parameter space of prime and prime-power dimensional entangled states (the dimensions where $d+1$ MUBs are known), and optimize our maximum complementarity protocol to find the states where the detection of entanglement via $2 - I_{d+1}$ is strongest:

$$\min_{q_i, \rho_d \geq 0, \rho_d^{TA} \geq 0} 2 - I_{d+1}[\rho_d] = \begin{cases} -0.15 (d=3) \\ -0.125 (d=4) \\ -0.106 (d=5) \\ -0.081 (d=7) \\ -0.073 (d=8) \\ -0.067 (d=9) \end{cases} \quad (8)$$

In each case, a similar geometry as shown in Fig. 3 is obtained. In dimension $d = 2 \cdot 3 = 6$ so far only 3 MUBs are found and there are strong numerical hints⁴¹ that there exist not more; applying only these does not lead to the detection of bound entanglement. In Ref.⁴² we have shown via geometry considerations that if a Hermitian operator detects entanglement of states in a certain quantum space \mathcal{W} , then it also detects entanglement in the multi-partite product space $\mathcal{W}^{\otimes n} := \{\rho_d^{\otimes n} = \sum c_{k,l} \tilde{P}_{k,l} | c_{k,l} \geq 0, \sum c_{k,l} = 1\}$. Also in this case, the d^2 Bell-type vertex states $\tilde{P}_{k,l}$ are obtained by applying a Weyl operator in one subsystem to $\tilde{P}_{0,0} = \frac{1}{d^2} \sum P_{k,l}^{\otimes n}$. Therefore, the maximum complementarity protocol is also applicable for multipartite states and can detect bound entanglement therein.

To illustrate the richness and difference between bipartite and multipartite entanglement, let us discuss first the famous case of $d = 2$. Then the vertex states are the Smolin states⁴³ that are known to be multiparticle un-lockable bound entangled, because no local party can distill entanglement; however, *two* parties can distill (unlock) the entanglement, which would in this case be actually a pure maximally entangled state; but it is only available for the other parties, not themselves. This case was recently experimentally demonstrated.^{2,3} Surprisingly, entangled states inside the magic simplex $\mathcal{W}^{\otimes n}$ can be distilled to the Smolin-type vertex states,⁴² which themselves are undistillable. For $d > 2$, in addition, the multipartite magic simplex contains *PPT*-entangled states, therefore, states that cannot even be purified to a vertex state. They are bound entangled and only “bound unlockable” due to their multiparticle nature.

We have proven experimentally that bipartite bound entanglement exists in Nature, which was predicted in 1998¹ and started an intensive theoretical quest in understanding its meaning. We have chosen orbital angular momentum entanglement of photons that is scalable in the dimensionality,¹⁴ and our high-quality results suggest that further exploration of high dimensional entangled quantum states is possible. Therefore, our experimental method and the maximum complementarity protocol is a useful addition to the toolbox to explore different types of entanglement including bound entanglement. With the case of two qutrits as the most simple system we lay the foundation to pursue the question why Nature should provide us with such a strange form of highly mixed entanglement that can not be purified, despite the fact we have used pure maximally entangled states as a resource to produce the state: What is its physical meaning? What are the quantum information theoretic applications of high-dimensional bound entanglement?

Finally, via the maximum complementarity protocol we provide an alternative proof that the maximum number

of mutually unbiased bases (MUBs) cannot be more than $d+1$: If for families of states that are optimally detected by I_{d+1} , another MUB would be added, we would detect separable states as entangled ones. The minimum number of existing MUBs is known to be the smallest of the prime factors of $d+1$. It is also open whether one always needs all MUBs to detect bound entanglement. Consequently, investigating inseparability problems opens a different trail to look for a solution of the number problem of MUBs.

Methods:

Maximum complementarity protocol. As an explicit example we show our choice of basis vectors of the four mutually unbiased bases \mathcal{B}_k with $w = e^{\frac{2\pi i}{3}}$:

$$\begin{aligned}\mathcal{B}_1 : \{|0_1\rangle, |1_1\rangle, |2_1\rangle\} &= \left\{ \begin{pmatrix} 1 \\ 0 \\ 0 \end{pmatrix}, \begin{pmatrix} 0 \\ 1 \\ 0 \end{pmatrix}, \begin{pmatrix} 0 \\ 0 \\ 1 \end{pmatrix} \right\} \\ \mathcal{B}_2 : \{|0_2\rangle, |1_2\rangle, |2_2\rangle\} &= \left\{ \begin{pmatrix} 1 \\ 1 \\ 1 \end{pmatrix}, \begin{pmatrix} 1 \\ w \\ w^2 \end{pmatrix}, \begin{pmatrix} 1 \\ w^2 \\ w \end{pmatrix} \right\} \\ \mathcal{B}_3 : \{|0_3\rangle, |1_3\rangle, |2_3\rangle\} &= \left\{ \begin{pmatrix} 1 \\ w \\ w \end{pmatrix}, \begin{pmatrix} 1 \\ w^2 \\ 1 \end{pmatrix}, \begin{pmatrix} 1 \\ 1 \\ w^2 \end{pmatrix} \right\} \\ \mathcal{B}_4 : \{|0_4\rangle, |1_4\rangle, |2_4\rangle\} &= \left\{ \begin{pmatrix} 1 \\ w^2 \\ w^2 \end{pmatrix}, \begin{pmatrix} 1 \\ 1 \\ w \end{pmatrix}, \begin{pmatrix} 1 \\ w \\ 1 \end{pmatrix} \right\}\end{aligned}$$

To detect (bound) entanglement, we choose the following combination of correlation functions $\langle |i^*\rangle = |i\rangle^*$:

$$\begin{aligned}C_{A_1, B_1} &= \sum_{i=0}^2 \text{Tr}(|i_1, \text{mod}(i_1+1, 3)^*\rangle \langle i_1, \text{mod}(i_1+1, 3)^*| \rho_3) \\ C_{A_k, B_k} &= \sum_{i=0}^2 \text{Tr}(|i_k, i_k^*\rangle \langle i_k, i_k^*| \rho_3), \quad k = 2, 3, 4.\end{aligned}$$

Experiment. We generate the spatially entangled photon pairs by collinear Type-I SPDC in a PPKTP crystal (length $L = 2$ mm) of a LG_0^0 laser beam (Kr^+ , $\lambda = 413$ nm, beam waist at crystal $w_p = 325$ μm , 80 mW power). The temperature is tuned to detect a similar amount of downconverted photons in the $\ell = 0$ and $\ell = \pm 1$ OAM mode. We image the crystal surface with $7.5\times$ magnification using a telescope onto the SLM (Hamamatsu X10468-07) surface. The SLM is operated under an incident angle of 10 or 5 degrees; this allows us to use a single SLM for both signal and idler photon.

The (phase-corrected) SLM is used with a blaze angle of 1 mrad. The elimination of the zeroth order is done in a time-reversed fashion *before* the SLM with a pinhole in the far field of the crystal behind L1 (Fig. 2). The far field of the SLM surface is sent to the single mode fibre using $10\times$ objectives, with a detection-fibre mode waist at the SLM of 1275 μm . The fibres are connected to single-photon counters and we post-select photon pairs by coincidence detection (time window 7 ns). All measurements were integrated for 2 s; we obtain typically 30,000 single counts and 1,500 coincidence counts for conjugated-field detector settings and <10 coincidence counts for the cases where no coincidences are expected. The SLM kinoforms required for 2-state superpositions involve only phase modulation, however, for 3-state superpositions such as those used for implementation of the maximum complementarity protocol, require spatial amplitude modulation, too. Because this is very inefficient if done in a continuous way,¹⁴ we employ binary amplitude modulation by removing the blaze at spatial positions where the normalized modulus of the detection field amplitude is smaller $\sqrt{0.5}$. For tomographic reconstruction, we obtain an overcomplete set of measurements by detecting all two-state superpositions with relative phases of $\{0, \pi/2, \pi, 3\pi/2\}$.

Supplementary information:

Phase space of two qutrits. Below, in Fig. 5, the finite phase space of the magic simplex³² is drawn for dimension $d = 3$. This space is spanned by all nine Bell states $P_{k,l}$, which can be generated by applying the Weyl operators $W_{k,l}$ onto one arbitrary maximally entangled Bell state, denoted by $P_{0,0}$: $P_{k,l} = W_{k,l} \otimes \mathbb{1} P_{0,0} W_{k,l}^\dagger \otimes \mathbb{1}$. Due to the group structure of the Weyl operators certain mixtures of the Bell states $P_{k,l}$ are geometrically equivalent, i.e. have the same properties concerning separability, bound entanglement, free entanglement and nonlocality (violation of a given Bell inequality). Thus one has not to analyze all possible mixtures since some are equivalent concerning the properties we are interested in. In particular, the so called *lines* are special. A line is formed by choosing one Bell state, e.g. $P_{0,0}$, and applying to it $d-1$ times the same Weyl operator, e.g. $W_{0,1}$. Applying another time the Weyl operator brings one back to to original state (in our case $P_{0,0}$), because of the periodicity of the Weyl operators. In our case the three Bell states $\{P_{0,0}, P_{0,1}, P_{0,2}\}$ form a line in the phase space (see Fig. 5). We find $d+1$ lines with different orientations through one Bell state $P_{0,0}$ (red lines in Fig. 5). To each (red) line there are 3 parallel lines. In summary, we find $(3+1) \times 3 = 12$ lines, which have the same geometry regarding separability, bound entanglement, free entanglement, and nonlocality.

For our state ρ_3 (Eq. 7), we see that the states weighted by q_1 and q_2 form a line and q_3 is the coefficient for another line that is parallel to the first one. Thus, we have

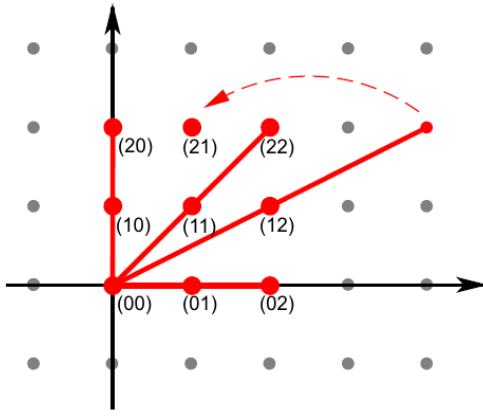


FIG. 5. Illustration of the finite discrete classical phase space for dimension $d = 3$ of the locally maximally mixed states of the magic simplex \mathcal{W} . Each point (kl) represent one of the nine Bell states $P_{k,l}$. All possible complete lines through the point (00) for $d = 3$ are drawn, representing one class of states which have the same geometry concerning separability, bound entanglement, free entanglement and nonlocality, i.e., those that are unitary equivalent. The same holds for each line which is parallel to any red line.

$(3+1) \times 3$ possibilities to choose a line and 3 possibilities to weight them with q_1 and q_2 . And there are 2 possibilities to choose parallel lines to the chosen one weighted by q_3 . Thus we have in total $(3+1) \times 3 \times 3 \times 2 = 72$ unitary equivalent possibilities to obtain the state ρ_3 , and all of these have in theory the same geometry regarding separability, bound entanglement, free entanglement and nonlocality.

In the experiment, the nine Bell states are not fully unitary equivalent due to wavefront errors, thus we get for all 72 possibilities slightly different values that allows to perform statistical analysis to obtain the true experimental errors for the complementarity protocol $2 - I_{d+1}$ and the minimum eigenvalue of the partial transpose $\text{Min}[\text{eig}(\rho^{T_A})]$.

Acknowledgements

We thank R.A. Bertlmann and A. Gabriel for discussions and acknowledge the SoMoPro programme, NWO, Austrian Science Fund (FWF-P23627-N16), and the EU STREP program 255914 (PHORBITECH). The Project is funded from the SoMoPro programme. Research of B.C.H. leading to these results has received a financial contribution from the European Community within the Seventh Framework Programme (FP/2007-2013) under Grant Agreement No. 229603. The research is also co-financed by the South Moravian Region. W.L. acknowledges support from NWO and the EU STREP program 255914 (PHORBITECH).

REFERENCES

- [1] Horodecki, M., Horodecki, P. & Horodecki, R. Mixed-State Entanglement and Distillation: Is there a “Bound” Entanglement in Nature? *Phys. Rev. Lett.* **80**, 5239 (1998).
- [2] Amselem, E. & Bourennane, M. Experimental four-qubit bound entanglement. *Nature Phys.* **5**, 748 (2009).
- [3] Lavoie, J., Kaltenbaek, R., Piani, M. & Resch, K. J. Experimental Bound Entanglement in a Four-Photon State. *Phys. Rev. Lett.* **105**, 130501 (2010).
- [4] Kaneda, F. *et al.* Experimental Activation of Bound Entanglement. *Phys. Rev. Lett.* **109**, 040501 (2012).
- [5] Barreiro, J. T. *et al.* Experimental multiparticle entanglement dynamics induced by decoherence. *Nature Phys.* **6**, 943 (2010).
- [6] Kampermann, H., Bruß, D., Peng, X. & Suter, D. Experimental generation of pseudo-bound-entanglement. *Phys. Rev. A* **81**, 040304 (2010).
- [7] DiGuglielmo, J. *et al.* Experimental Unconditional Preparation and Detection of a Continuous Bound Entangled State of Light. *Phys. Rev. Lett.* **107**, 240503 (2011).
- [8] Brunner, N. & Cavalcanti, D. Quantum steering with bound entanglement. *pre-print* (2012). 1210.1556v1.
- [9] Epping, M. & Brukner, C. Bound entanglement useful for reducing communication complexity. *pre-print* (2012). 1209.2962.
- [10] Lavoie, J., Kaltenbaek, R., Piani, M. & Resch, K. J. Experimental bound entanglement? *Nature Phys.* **6**, 827 (2010).
- [11] Allen, L., Beijersbergen, M. W., Spreeuw, R. J. C. & Woerdman, J. P. Orbital angular momentum of light and the transformation of Laguerre-Gaussian laser modes. *Phys. Rev. A* **45**, 8185 (1992).
- [12] Molina-Terriza, G., Torres, J. P. & Torner, L. Twisted photons. *Nature Phys.* **3**, 305 (2007).
- [13] Mair, A., Vaziri, A., Weihs, G. & Zeilinger, A. Entanglement of the orbital angular momentum states of photons. *Nature* **412**, 313 (2001).
- [14] Dada, A. C., Leach, J., Buller, G. S., Padgett, M. J. & Andersson, E. Experimental high-dimensional two-photon entanglement and violations of generalized Bell inequalities. *Nature Phys.* **7**, 677 (2011).
- [15] Salakhutdinov, V. D., Eliel, E. R. & Löffler, W. Full-Field Quantum Correlations of Spatially Entangled Photons. *Phys. Rev. Lett.* **108**, 173604 (2012).
- [16] Shalm, L. K. *et al.* Three-photon energy-time entanglement. *Nature Phys.* **advance online publication**, (2012).
- [17] Bechmann-Pasquinucci, H. & Peres, A. Quantum Cryptography with 3-State Systems. *Phys. Rev. Lett.* **85**, 3313 (2000).
- [18] Kaszlikowski, D., Gnaniński, P., Żukowski, M., Miklaszewski, W. & Zeilinger, A. Violations of Local Realism by Two Entangled N -Dimensional Systems Are Stronger than for Two Qubits. *Phys. Rev. Lett.* **85**, 4418 (2000).
- [19] Fujiwara, M., Takeoka, M., Mizuno, J. & Sasaki, M. Exceeding the Classical Capacity Limit in a Quantum Optical Channel. *Phys. Rev. Lett.* **90**, 167906 (2003).
- [20] Bechmann-Pasquinucci, H. & Tittel, W. Quantum cryptography using larger alphabets. *Phys. Rev. A* **61**, 062308 (2000).

- [21] Peres, A. Separability Criterion for Density Matrices. *Phys. Rev. Lett.* **77**, 1413 (1996).
- [22] Horodecki, M., Horodecki, P. & Horodecki, R. Separability of mixed states: necessary and sufficient conditions. *Phys. Lett. A* **223**, 1 (1996).
- [23] Sanpera, A., Tarrach, R. & Vidal, G. Local description of quantum inseparability. *Phys. Rev. A* **58**, 826 (1998).
- [24] Bell, J. Bertlmann's socks and the nature of reality. *J. Phys. Colloques* **42**, 2 (1981).
- [25] Spengler, C., Huber, M., Brierley, S., Adaktylos, T. & Hiesmayr, B. C. Entanglement detection via mutually unbiased bases. *Phys. Rev. A* **86**, 022311 (2012).
- [26] Hiesmayr, B. C., Huber, M. & Krammer, P. Two computable sets of multipartite entanglement measures. *Phys. Rev. A* **79**, 062308 (2009).
- [27] Huber, M., Mintert, F., Gabriel, A. & Hiesmayr, B. C. Detection of High-Dimensional Genuine Multipartite Entanglement of Mixed States. *Phys. Rev. Lett.* **104**, 210501 (2010).
- [28] Gabriel, A., Hiesmayr, B. & Huber, M. Criterion for K-separability in mixed multipartite states. *Quantum Inf. Comput.* **10**, 829 (2010).
- [29] Monken, C. H., Ribeiro, P. H. S. & Pádua, S. Transfer of angular spectrum and image formation in spontaneous parametric down-conversion. *Phys. Rev. A* **57**, 3123 (1998).
- [30] Franke-Arnold, S., Barnett, S. M., Padgett, M. J. & Allen, L. Two-photon entanglement of orbital angular momentum states. *Phys. Rev. A* **65**, 033823 (2002).
- [31] Walborn, S. P., de Oliveira, A. N., Thebaldi, R. S. & Monken, C. H. Entanglement and conservation of orbital angular momentum in spontaneous parametric down-conversion. *Phys. Rev. A* **69**, 023811 (2004).
- [32] Baumgartner, B., Hiesmayr, B. C. & Narnhofer, H. State space for two qutrits has a phase space structure in its core. *Phys. Rev. A* **74**, 032327 (2006).
- [33] Baumgartner, B., Hiesmayr, B. & Narnhofer, H. A special simplex in the state space for entangled qudits. *J. Phys. A* **40**, 7919 (2007).
- [34] Baumgartner, B., Hiesmayr, B. & Narnhofer, H. The geometry of bipartite qutrits including bound entanglement. *Phys. Lett. A* **372**, 2190 (2008).
- [35] Bertlmann, R. A. & Krammer, P. Entanglement witnesses and geometry of entanglement of two-qutrit states. *Ann. Phys.* **324**, 1388 (2009).
- [36] Acin, A. Entanglement: Entangled and bound. *Nature Phys.* **5**, 711 (2009).
- [37] Dobek, K., Karpiński, M., Demkowicz-Dobrzański, R., Banaszek, K. & Horodecki, P. Experimental Extraction of Secure Correlations from a Noisy Private State. *Phys. Rev. Lett.* **106**, 030501 (2011).
- [38] Peters, N. A. *et al.* Maximally Entangled Mixed States: Creation and Concentration. *Phys. Rev. Lett.* **92**, 133601 (2004).
- [39] Puentes, G., Voigt, D., Aiello, A. & Woerdman, J. P. Tunable spatial decoherers for polarization-entangled photons. *Opt. Lett.* **31**, 2057 (2006).
- [40] James, D. F. V., Kwiat, P. G., Munro, W. J. & White, A. G. Measurement of qubits. *Phys. Rev. A* **64**, 052312 (2001).
- [41] Durt, T., Englert, B., Bengtsson, I. & Życzkowski, K. On mutually unbiased bases. *Int. J. Quantum Inf.* **8**, 535 (2010).
- [42] Hiesmayr, B. C. & Huber, M. Two distinct classes of bound entanglement: PPT-bound and 'multi-particle'-bound. *pre-print* (2009). 0906.0238.
- [43] Smolin, J. A. Four-party unlockable bound entangled state. *Phys. Rev. A* **63**, 032306 (2001).